



ANALYSIS OF REINFORCED CONCRETE HOLLOW PIERS BEHAVIOR: BENEFITS OF FRP CONFINEMENT

Gian Piero Lignola¹, Andrea Prota¹, Gaetano Manfredi² and Edoardo Cosenza²
Department of Structural Engineering, University of Naples, Naples, Italy

Received 13 November 2008

Revised 21 February 2009

Accepted 17 March 2009

Reliable stress-strain behavior of concrete is necessary particularly when a member is subjected to combine bending and axial load and confinement effects should be accounted for. A unified theory for confinement of circular hollow sections is proposed herein, that can be extended to the case of solid and noncircular sections. The main aim of the model is to trace step-by-step the evolution of the three dimensional stresses in confined concrete and confining devices (i.e. FRP externally bonded jackets). The iterative model is able to estimate confinement effectiveness and to plot stress-strain relationships, which are different in the case of solid and hollow sections. Through the proposed improved model, a simplified closed form solution has been also derived to directly determine ultimate confined concrete properties and stress-strain curves. At present, theoretical results based on the proposed concrete circular hollow sections confinement model, in satisfactory agreement with the experimental data available in scientific literature, show that FRP jacketing can enhance the ultimate load and ductility significantly, also in the case of hollow concrete cross sections.

Keywords: modeling, hollow sections, concrete confinement, nonlinear analysis

1. Introduction

Column jacketing with Fiber Reinforced Polymer (FRP) composite materials has been extensively studied in recent years but it is uncertain how FRP jackets may perform retrofitting hollow concrete columns since the topic has been scantily researched. Hollow reinforced concrete (RC) bridge piers are used in tall bridges to maximize the structural efficiency of the strength-

¹ Assistant Professor

² Professor

mass and stiffness-mass ratios. Few studies to date have covered circular and rectangular hollow columns: a review can be found in Lignola et al. (2007a) regarding columns with applied low levels of axial load, investigating the performance of the cross sections subjected to combined shear and flexure stresses. The assessment of such type of RC structures especially requires advanced tools: tension stiffening effect, compressed bars buckling, concrete cover spalling and FRP confinement of concrete should be included to model hollow members (Lignola et al. 2007b). Plane strain conditions were adopted to simulate the confinement effect; Braga et al. (2006) proposed a model for solid sections based on the assumption that the increment of stress in the concrete is achieved without any out-of-plane strain. A model based on equilibrium and radial displacement compatibility, has also been presented (Fam and Rizkalla 2001a, Eid and Paultre 2007) adopting the equations proposed by Mander et al. (1988) through a step-by-step strain increment technique to trace the lateral dilation of concrete.

2. Mathematical Model

2.1. Confinement Model

The passive confinement on axially loaded concrete members is due to the transverse dilation of concrete and the presence of a confining device which opposes this expansion and puts the concrete in a triaxial state of stress. The failure of the confined concrete member is due to the rupture of the FRP confinement which is controlled by a multiaxial criterion -i.e. Tsai-Wu failure criteria adopted in an effective ultimate strain prediction model (Lignola et al. 2008a).

The dependence of the lateral pressure with the axial strain is explicitly considered through radial equilibrium equations and displacement compatibility (details on the base model can be found in Lignola et al. 2008b). Assuming axial symmetry, the radial displacement is the only displacement component and stress components σ_r and σ_θ (where r calls for the radial component and θ for the circumferential component) can be evaluated according to boundary conditions, e.g. applied external (at $r = R_c$) inward pressure q_e .

In the case of external inward pressure, q_e , the stress equations become (Lignola et al. 2008b):

$$\sigma_r = \frac{q_e R_c^2}{R_c^2 - R_i^2} \left(1 - \frac{R_i^2}{r^2} \right) \quad (1a)$$

$$\sigma_\theta = \frac{q_e R_c^2}{R_c^2 - R_i^2} \left(1 + \frac{R_i^2}{r^2} \right) \quad (1b)$$

$$s_r(r) = \frac{1+\nu_c}{E_c} \frac{q_e R_e^2}{R_e^2 - R_i^2} \left[(1-2\nu_c)r + \frac{R_i^2}{r} \right] \quad (1c)$$

where R_i is the internal radius. The circumferential and radial stress fields in the hollow cylinder are depicted in Figures 1(a) and 1(b), respectively.

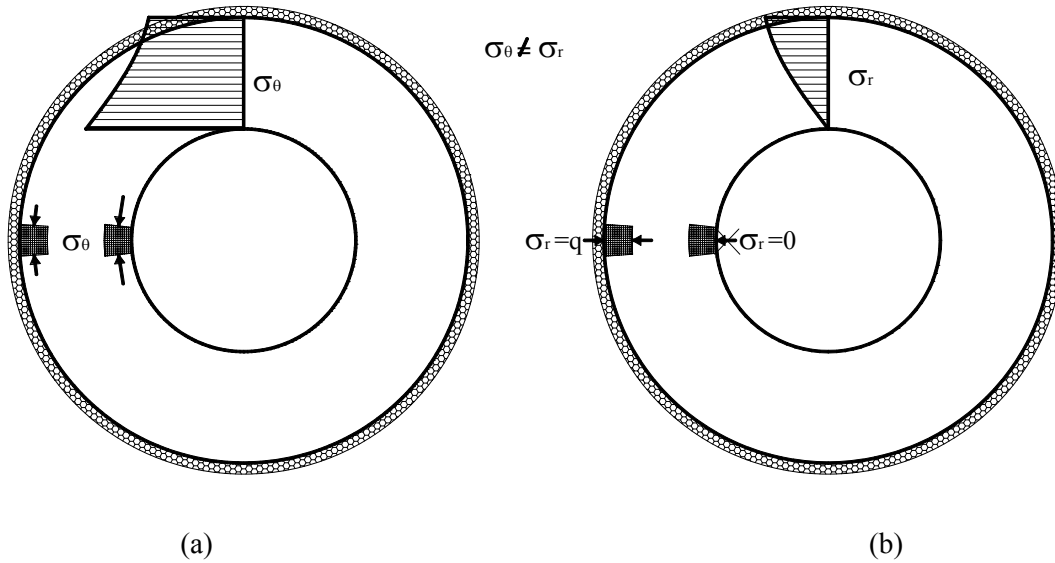


Figure 1. Stress fields in hollow cylinders: a) circumferential component; b) radial component

In the case of a thin FRP jacket where the thickness $t \ll R_e$, loaded by an internal outward pressure q_i , the stress and displacement equations can be simplified as:

$$\sigma_{\theta,FRP} \approx -\frac{q_i R_e}{t} \quad (2a)$$

$$s_{r,FRP}(r) \approx -\frac{q_i R_e^2}{E \cdot t} (1-\nu_f) \quad (2b)$$

The sum of the radial displacements of concrete (the expansion due to axial load, $s_c = -R_e \cdot \nu_c \cdot \epsilon_c$, and the contraction due to confining pressure, Equation. (1c)) is equal to the device expansion due to the outward confined concrete pressure, Equation. (2b), according to Figure 2. Besides, the confining device is in equilibrium with the concrete cylinder so that the inward pressure q_i on concrete cylinder is equal to the outward pressure $q_e = -q_i = q$ on the confining jacket.

All the previous equations can be explicated in the form $q=q(\epsilon_c)$, so that, at each axial strain ϵ_c , the confining pressure q exerted on concrete by the FRP jacket is associated to:

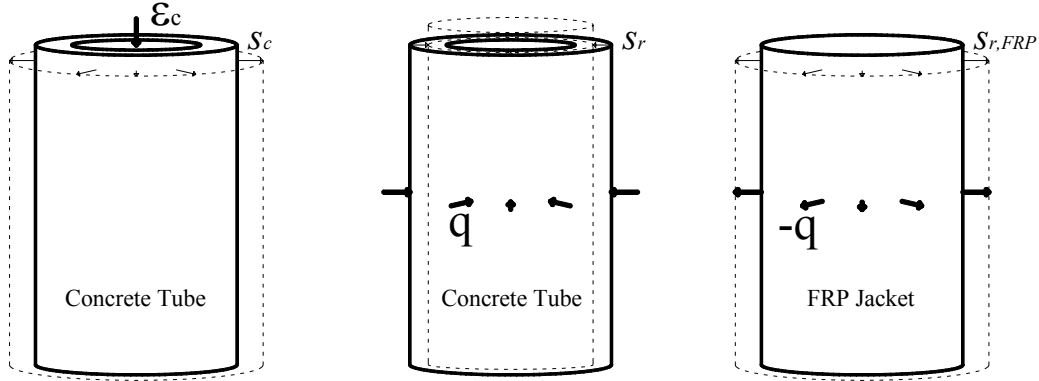


Figure 2. Radial displacement contributions of concrete tube and FRP Jacket

$$q = \frac{\nu_c}{\frac{R_e}{E_{ft}}(1-\nu_f) + \frac{1+\nu_c}{E_c} \frac{R_e^2}{R_e^2-R_i^2} \left[(1-2\nu_c) + \left(\frac{R_i}{R_e} \right)^2 \right]} \epsilon_c \quad (3)$$

Adopted symbols are clarified in Figure 3. The key aspect of the proposed model for hollow core sections is the different contribution of radial and circumferential stresses explicitly considered through a plasticity model for concrete under triaxial compression. The confining stress field is not equal in the two transverse directions and the effect of confinement is evaluated in each circular crown of the cross-section where the effective confining pressures differ in the two orthogonal directions (radial and circumferential).

Previous equations are based on linear elasticity, plain strain, theory for all the involved materials (E_c , ν_c and E_f , ν_f are elastic modulus and Poisson's ratio for concrete and FRP, respectively). This assumption is exactly true for the elastic confining device (i.e. FRP), while, as axial deformation increases, the concrete exhibits a nonlinear behavior characterized by the appearance of significant cracking and it shows an increase in the (apparent) Poisson's ratio and a decrease in the elastic modulus. To account for the nonlinear behavior of concrete, a secant approach can be considered: to simplify and avoid an iterative procedure to determine the actual $E_c(\epsilon_c)$, the secant modulus of the iteration (i) is assumed as the secant modulus, that is the slope of the line

connecting the origin with the previously evaluated stress-strain point (i-1) on the confined concrete stress-strain curve. It is highlighted that the influence of axial strain, ϵ_c , increment step size is almost negligible (e.g. reducing the step size from 0.24% to 0.04%, the confined concrete stress-strain curve changes by less than approximately 0.5%).

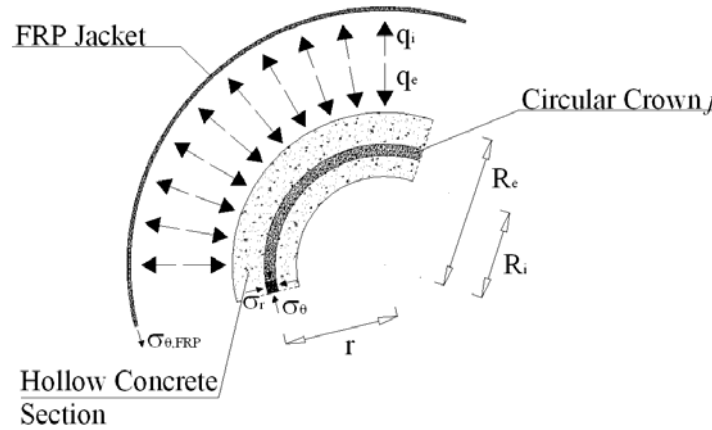


Figure 3. Symbols and boundary conditions (exploded view)

The lateral-to-axial strain relationship provides the essential connection between the response of the concrete column and the response of the FRP jacket in a passive-confinement model for FRP-confined concrete (Jiang and Teng 2007). An absolute value of the secant slope of the lateral-to-axial strain curve of FRP-confined concrete, $\nu_c = \epsilon_\theta / \epsilon_c$, applicable to unconfined, actively confined and FRP-confined concrete was proposed by Teng et al. (2007) in the form:

$$\frac{\epsilon_c}{\epsilon_{co}} = 0.85 \left(1 + 8 \frac{f'_l}{f'_{co}} \right) \left[\left(1 + 0.75 \frac{\epsilon_\theta}{\epsilon_{co}} \right)^{0.7} - e^{-\frac{7\epsilon_\theta}{\epsilon_{co}}} \right] \quad (4)$$

In the above Equation (4), ϵ_{co} is the unconfined peak concrete strain; usually it is set equal to 0.002, and f'_{co} is the corresponding stress (strength). Only at this stage a single confining stress, f'_l , is assumed as the average of the two, radial and circumferential, components, and it results constant with respect to the radial position r :

$$f'_i = \frac{\sigma_r + \sigma_\theta}{2} = q \frac{R_e^2}{R_e^2 - R_i^2} = \frac{v_c}{\frac{(1-v_f)(R_e^2 - R_i^2)}{E_f t R_e} + \frac{1+v_c}{E_c} \left[(1-2v_c) + \left(\frac{R_i}{R_e} \right)^2 \right]} \varepsilon_c \quad (5)$$

In Equation (4) the only unknown, ε_θ , is iteratively evaluated (See Figure 4 for a flowchart of the iterative procedure) at each step i , for any given axial strain, ε_c .

A first trial value of the Poisson's ratio and of the elastic modulus is determined for concrete (e.g. the initial elastic Poisson's ratio, usually ranging between 0.1 and 0.3, and the initial elastic modulus evaluated according to ACI 318M-02 as $4700\sqrt{f'_{co}}$, at the beginning of the procedure or their previously evaluated values at iteration $i-1$). This Poisson's ratio allows to evaluate $\varepsilon_\theta = \varepsilon_c \cdot v_c$, and it is adopted in Equations (3) and (5) to evaluate f'_i and in turn to evaluate a new value ε_c - Equation. (4). The procedure is repeated changing ε_c up to a value such that the emerging value ε_c in output converges to the given axial strain, ε_c , in input at step i . Then it is possible to evaluate for each circular crown j , in which the hollow circular cross section can be divided, the confined concrete vertical strength depending on the radial and circumferential confining pressures - given by Equations (1a) and (1b) where r refers to the centerline of the circular crown j . The final value of the confined concrete strength, f_{cc} , is the weighted average over the concrete section, and rather refined values of f_{cc} are provided even dividing the section only in few circular crowns.

2.2. Plasticity model for Concrete

The ultimate strength surface is formulated in the Haigh–Westergaard stress space defined by the cylindrical coordinates of hydrostatic length (ξ), deviatoric length (ρ) and Lode angle (θ).

These coordinates are functions of the invariants (I_1, J_2, J_3) of the principal stress tensor components: $\sigma_1 (= \sigma_r) < \sigma_2 (= \sigma_\theta) < \sigma_3 (= f_{cc})$, according to the following equations:

$$\xi = \frac{I_1}{3} \quad I_1 = \sigma_1 + \sigma_2 + \sigma_3 \quad (6a)$$

$$\rho = \sqrt{\frac{2J_2}{5}} \quad J_2 = \frac{1}{6} [(\sigma_1 - \sigma_2)^2 + (\sigma_2 - \sigma_3)^2 + (\sigma_3 - \sigma_1)^2] \quad (6b)$$

$$\cos \theta = \frac{3\sqrt{3}}{2} \frac{J_3}{J_2^{3/2}} \quad J_3 = \left(\sigma_1 - \frac{I_1}{3} \right) \left(\sigma_2 - \frac{I_1}{3} \right) \left(\sigma_3 - \frac{I_1}{3} \right) \quad (6c)$$

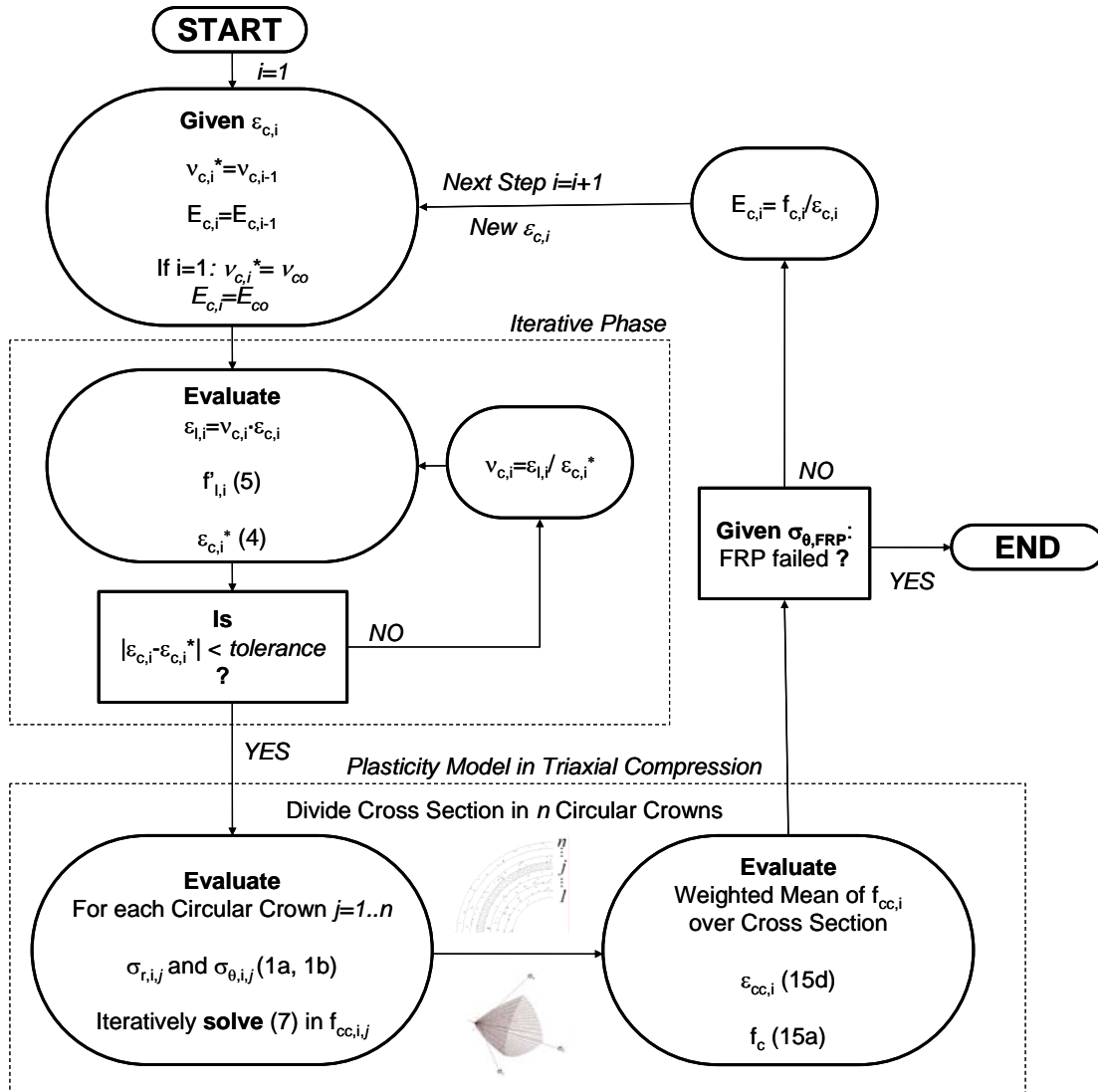


Figure 4. Flow Chart of the proposed hollow section confinement model

William and Warnke (1975) have proposed the equations for defining the ultimate concrete strength surface (Figure 5a). The Rendulic and deviatoric views of the surface are shown in Figures 5b and 5c, respectively. The surface has curved meridians and the generators are approximated by second-order parabolas along $\theta=0^\circ$ (tensile meridian) and $\theta=60^\circ$ (compressive meridian) with a common apex at the hydrostatic axis. The failure of concrete is predicted if the state of stress satisfies the condition:

$$\rho = r(\theta, \xi) \cdot f'_{co} \quad (7)$$

Where:

$$r(\theta, \xi) = \frac{2r_c(r_c^2 - r_t^2)\cos\theta + r_c(2r_t - r_c)\sqrt{4(r_c^2 - r_t^2)\cos^2\theta + 5r_t^2 - 4r_c r_t}}{4(r_c^2 - r_t^2)\cos^2\theta + (2r_t - r_c)^2} \quad (8a)$$

$$\cos\theta = \frac{2\sigma_1 - \sigma_2 - \sigma_3}{\sqrt{12J_2}} \quad (8b)$$

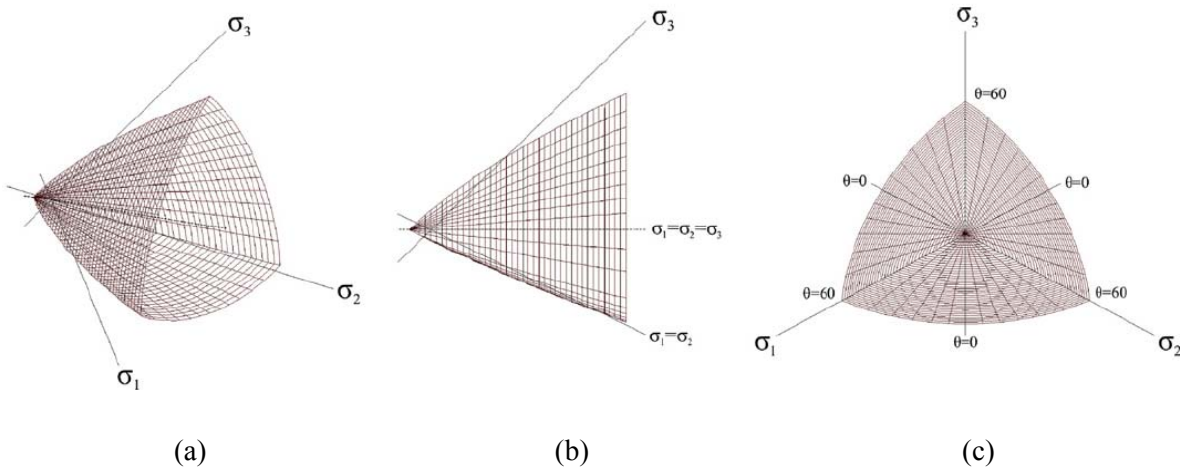


Figure 5. a) Ultimate strength surface; b) in the Rendulic plane; c) in the deviatoric plane

The parabolic meridians r_c and r_t are the control parameters; they were calibrated by Elwi and Murray (1979) on five control points based on Schikert-Winkler (1977) experimental data and they are expressed as:

$$r_c = 0.095248 + 0.891175\left(\frac{\xi}{f'_{co}}\right) - 0.244420\left(\frac{\xi}{f'_{co}}\right)^2 \quad (9a)$$

$$r_t = 0.053627 + 0.512079\left(\frac{\xi}{f'_{co}}\right) - 0.038226\left(\frac{\xi}{f'_{co}}\right)^2 \quad (9b)$$

In Equation (7) the only unknown is $\sigma_3=f_{cc}$ and it is iteratively evaluated. The iterative procedure is repeated for every couple of confining stresses in the circular crowns j, $\sigma_1=\sigma_r$ and $\sigma_2=\sigma_\theta$. A first

trial value for σ_3 is determined (e.g. the unconfined concrete strength f'_{co} or the f_{cc} evaluated in previous circular crown). The procedure is repeated changing σ_3 up to a value such that Equation (7) is satisfied. Section 3.1 describes last steps of the proposed procedure to plot stress-strain curves.

It is noted that the cited model is the basis for the equation reported, for instance, in the ACI 440.2R (2002) code to evaluate the cylindrical confined concrete strength $f_{cc,TRIAX} = \sigma_3$, given a uniform confining pressure $\sigma_1 = \sigma_2 = f'_1$, leading to the well known equation:

$$f_{cc,TRIAX} = f'_c \left(2.25 \sqrt{1 + 7.9 \frac{f'_1}{f'_c}} - 2 \frac{f'_1}{f'_c} - 1.25 \right) \quad (10)$$

3. Simplified Closed Form Solution for Concrete Confinement

At this point, an alternative simplified approach is shown, that gives rather accurate results despite the heavily reduced computational effort (no iterations are needed). The concrete contraction contribution related to the elastic modulus is neglected and the confining stress field is simplified: the variations of σ_θ and σ_r along the radius are neglected. On safe side, their smallest values are considered: σ_θ has a minimum for $r=R_e$ in Equation (1b), while σ_r , ranging between zero at $r=R_i$ and q at $r=R_e$, is assumed zero.

After a regression analysis of Equation (7) where simplified assumptions lead to $\sigma_1=0$ and $\sigma_2=f'_1$, the following equation is proposed:

$$\frac{f_{cc}}{f'_{co}} = 1 + 2,3644 \frac{f'_1}{f'_{co}} - 7,7246 \left(\frac{f'_1}{f'_{co}} \right)^2 + 15,832 \left(\frac{f'_1}{f'_{co}} \right)^3 - 18,447 \left(\frac{f'_1}{f'_{co}} \right)^4 + 10,932 \left(\frac{f'_1}{f'_{co}} \right)^5 - 2,6128 \left(\frac{f'_1}{f'_{co}} \right)^6 \quad (11)$$

where $f'_1/f'_{co} < 1.35$. In the case of hollow cylinders with large wall thickness, $R_e - R_i$, compared to the radius, R_e , it is too conservative to adopt Equation (11) and a linear interpolation is suggested between the cited equation and Equation (10) referred to a tri-axial confined concrete with uniform confining pressure, according to the following:

$$f'_{cc} = f_{cc,TRIAx} \left(1 - \frac{R_i}{R_e} \right) + f_{cc} \left(\frac{R_i}{R_e} \right) \quad (12)$$

and Equation (12) converges to Equation (10) in the case of solid sections (where $R_i=0$). It is suggested to adopt the radial stress $f'_1 = \sigma_r$, equal to q at $r=R_e$, in Equations (10) and (11): these simplified assumptions lead to the form:

$$q = \left[\frac{E_f t}{R_e (1 - \nu_f)} \right] \cdot \nu_c \varepsilon_c = \left[\frac{E_f t}{R_e (1 - \nu_f)} \right] \cdot \varepsilon_\theta \quad (13)$$

The three parameters f'_1 equal to q in Equation (13), f'_{cc} in Equation (12) and ε_c in Equation (4) are expressed as a function of the lateral strain ε_θ if the mechanical properties of unconfined concrete and FRP, and the geometrical dimensions of the section are known. Equation (4) was established for solid sections; to adapt it to the case of hollow sections, it is suggested to consider the average confining stress field through Equation (5) modified to account for the simplified assumptions in:

$$f'_1 = \frac{\sigma_r + \sigma_\theta}{2} = q \frac{R_e^2}{R_e^2 - R_i^2} = \left[\frac{E_f t}{(1 - \nu_f)} \frac{R_e}{R_e^2 - R_i^2} \right] \cdot \nu_c \varepsilon_c = \left[\frac{E_f t}{(1 - \nu_f)} \frac{R_e}{R_e^2 - R_i^2} \right] \cdot \varepsilon_\theta \quad (14)$$

Once the axial strain ε_c function is known, it is possible to evaluate the corresponding stress f_c function through the procedure described in the next section. The key aspect is that the lateral strain ε_θ , ranging between zero and the jacket failure strain, is the driving parameter of these functions instead of the axial strain ε_c .

3.1. Stress-Strain Curve and Ultimate Properties of Confined Concrete

The stress-strain model of confined concrete proposed by Mander et al. (1988) has been adopted:

$$f_c = \frac{f_{cc} \cdot x \cdot p}{p - 1 + x^p} \quad (15a)$$

$$x = \varepsilon_c / \varepsilon_{cc} \quad (15b)$$

$$p = \frac{E_{co}}{E_{co} - f_{cc} / \varepsilon_{cc}} \quad (15c)$$

$$\varepsilon_{cc} = \varepsilon_{co} \left(5 \frac{f_{cc}}{f_{co}} - 4 \right) \quad (15d)$$

where ε_{cc} is the strain corresponding to confined concrete strength. A “Mander curve” –Equation (15a)- at a given constant confining pressure f_1 can be drawn and the “true” stress point f_c can be determined corresponding to the actual strain ε_c -Equation (15b). At each level of load/deformation (namely ε_c), the complete stress and strain regime in both the concrete cylinder and confining device is known, i.e. the circumferential stress in the confining device is given by Equation (2a). The procedure is repeated up to a value of axial strain that induces failure of the confining device. A suitable failure criterion should be incorporated to detect the confining device failure; e.g. when the circumferential stress in the jacket reaches its strength, or by adopting the novel model proposed in Lignola et al. (2008c) based on Tsai-Wu criterion (Daniel and Ishai 2006) for FRP, accounting for the triaxial state of stress in the jacket.

Following the proposed simplified model (Section 3), the ultimate properties of confined concrete can be easily evaluated once the maximum confinement stress, $f_1(\varepsilon_{FRP,u})$ (and corresponding ultimate FRP strain, $\varepsilon_{FRP,u}$) is given. Assuming that the ultimate strain of FRP jacket at failure, $\varepsilon_{FRP,u}$, is known, Equations (14) and (4) are solved to evaluate the ultimate axial strain of concrete $\varepsilon_{c,u}$. Hence, the corresponding stress is given by Equations (12) and (15).

4. Theoretical-Experimental Comparison

Experimental tests on FRP-confined concrete specimens with circular cross sections, available in the scientific literature, have been simulated according to the proposed confinement model to validate it. Specimens are wrapped with either carbon or glass fiber FRP composites. Some experimental campaigns include both solid and hollow cross-section specimens; these tests are considered to validate the proposed unified model for both types of sections. Some other test campaigns include only solid sections (made by either plain concrete or reinforced concrete) and

they have been considered by other authors as benchmarks for their concrete confinement models (Fam and Rizkalla 2001a, Spoelstra and Monti 1999). Each campaign is briefly described below; it is underlined that, for all presented comparisons, the Young Modulus of unconfined concrete has been derived from experimental curves, other materials data are provided in the following reports. In next plots, the theoretical predictions based on the refined iterative model are in solid lines, while the approximate predictions based on simplified direct method are in dashed lines.

4.1. Tests by Modarelli et al. (2005)

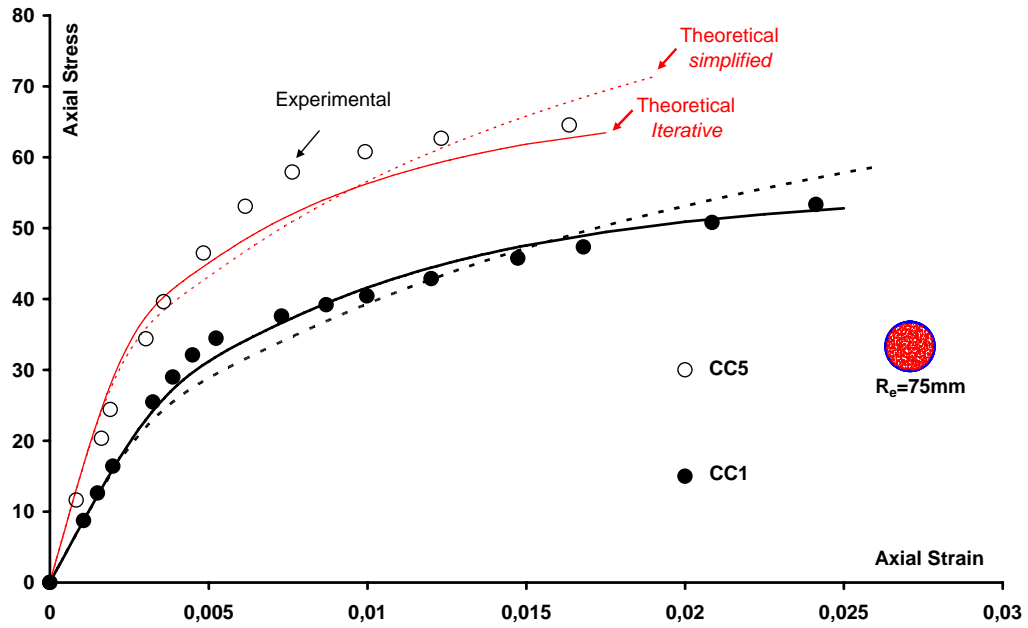
A set of 124 tests including 85 specimens wrapped with FRP and 39 plain concrete specimens was conducted. Two different kinds of concrete mixes were made to investigate the effect of the concrete: the average 28-day compressive strength was 28 MPa and 38 MPa respectively.

The specimens were 150 mm in diameter and 300 mm in height, and had different internal diameters (CC1 and CC5: 0 mm, which is solid section; CC2 and CC3: 50 mm).

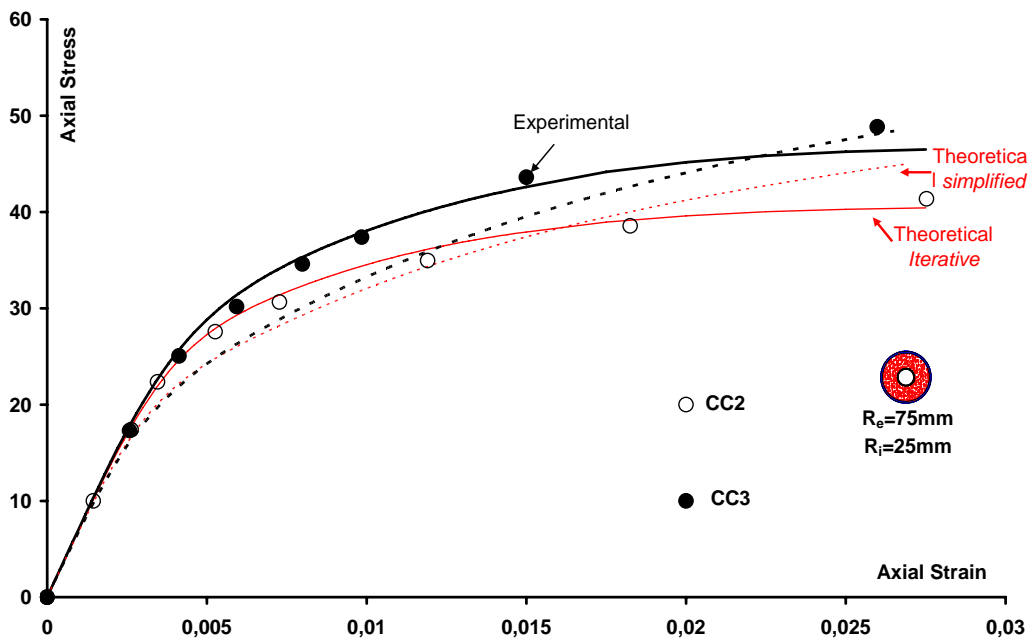
The concrete specimens were wrapped with unidirectional CFRP composites with 0.165 mm thickness, each ply. The CC2 and CC3 hollow specimens were wrapped with one and two plies, respectively. All the unidirectional CFRP composite jackets had fibers aligned at 90° to the principal axis of the specimen. Hoop strength was 3068 MPa and the Young Modulus was 221 GPa.

The response of these specimens was predicted and compared to the experimental outcomes in figures 6a-6b.

Satisfactory agreement was found between the measured values and the predicted response. An experimental peak concrete compressive strain, unconfined, ranging between 0.38% and 0.63% was considered.



(a)



(b)

Figure 6. Predicted response vs. experimental outcome: Modarelli et al. (2005)

4.2. Tests by Fam and Rizkalla (2001b)

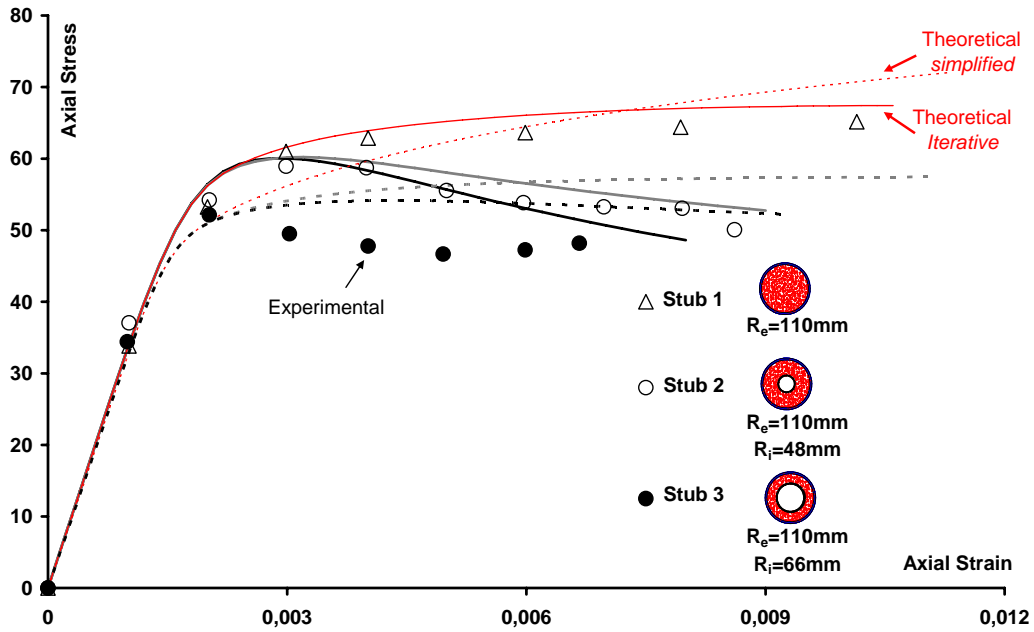
A set of three experiments on cylindrical hollow and solid plain concrete specimens confined with glass fiber tubes with different wall thicknesses were carried out. The specimens were 219 mm in external diameter and had different internal diameters (Stub 1: 0 mm that is solid section; Stub 2: 95 mm; Stub 3: 133 mm) with cylindrical compressive strength of 58 MPa.

The specimens were wrapped with a 33.4 GPa, Young Modulus glass fiber-reinforced polymer (CFRP) shell (2.21 mm thickness) with stacking sequence of nine layers $[-88/-88/+4/-88/-88/+4/-88/+4/-88]$ and tensile strength of 548 MPa. The stress versus axial strain response was predicted and compared to the measured values in figure 7a. Satisfactory agreement was found again between the measured values and the predicted response for the confined concrete compressive strength. A peak concrete compressive strain was estimated of 0.2%.

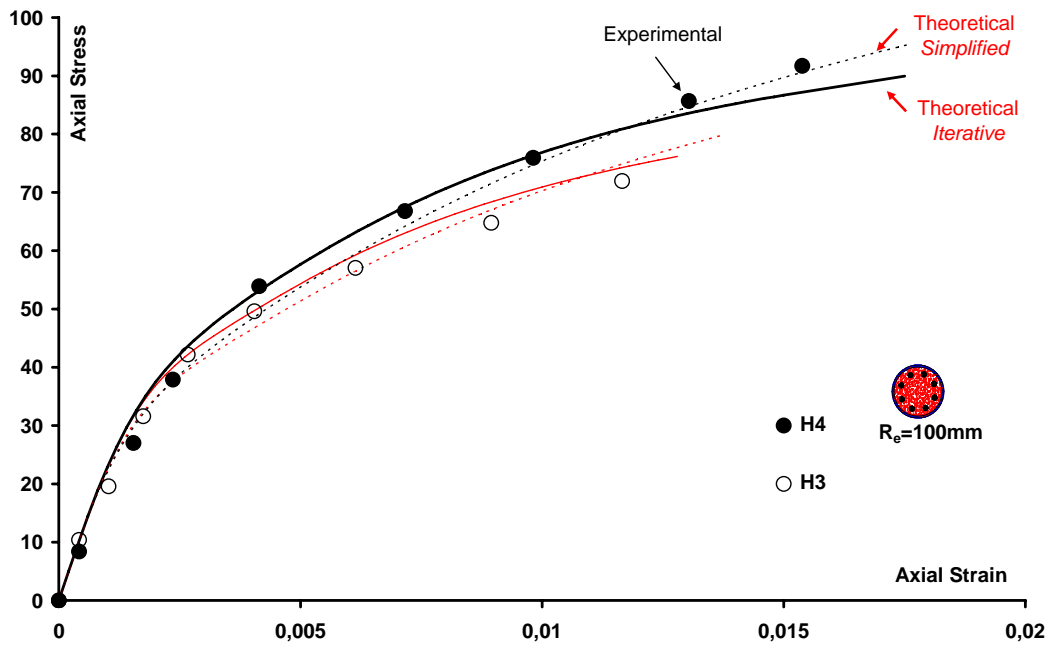
4.3. Tests by Kawashima et al. (1997)

Two 200 x 600 mm reinforced concrete specimens with 39 MPa concrete and wrapped with carbon fiber-reinforced polymer and tested under axial compression were simulated. These solid cylindrical specimens were provided with a longitudinal steel reinforcement ratio of 1%, with a yield stress of 295 MPa, whose contribution was subtracted from the experimentally measured stresses (Spoelstra and Monti 1999). The specimens, both of them with solid section, were wrapped with two different high-modulus carbon fiber-reinforced polymer sheets, with jacket thicknesses of 0.338 mm (H3) and 0.676 mm (H4) and tensile strengths of 2810 and 2327 MPa, respectively.

The Young Modulus of the jacket was 439 GPa. The stress versus axial strain response was properly predicted and it is compared to the measured values in figure 7b. The peak concrete compressive strain is 0.3%.



(a)



(b)

Figure 7. Predicted response vs. experimental outcome: a) Fam and Rizkalla (2001b); b) Kawashima et al. (1997)

5. Conclusions

The simplified model is derived from a more refined iterative confinement model proposed by the same authors (Lignola et al. 2008b). The iterative model has been also improved and it is able to predict the fundamentals of the behavior of hollow members confined with FRP both in terms of strength and ductility, giving a clear picture of the effectiveness of confinement on the response of this kind of elements. This model can be extended to the case of a solid section and, in this sense, is a unified model, able to trace the evolution of stresses and strains in the confinement wraps and concrete.

The larger the hole, the higher is the deformability of the element thus resulting, for a similar level of dilation, in different stress paths: in the case of a solid section the dilation of concrete is restrained by the FRP wraps and this interaction causes a strength enhancement, while in the case of thin walls, the greater deformability does not allow such strength improvement to be gained, even though significant ductility enhancement is achieved. In this case the state of stress becomes mostly circumferential.

The simplified closed form solution has been derived to determine directly the ultimate confined concrete properties and stress-strain curves. The simplified model gives rather accurate results despite the heavily reduced computational effort (no iterations are needed). The key aspect is that the driving parameter is the lateral strain ϵ_{θ} instead of the axial strain ϵ_c . At present, theoretical results, based on the improved iterative model or on the simplified assumptions, are in satisfactory agreement with the available experimental data and show that FRP jacketing can enhance ultimate load and ductility significantly also in the case of hollow concrete members.

References

- ACI Committee 318 (2002), “Building code requirements for structural concrete (ACI 318M-02)”, *American Concrete Institute*, Farmington Hills, USA.
- ACI Committee 440 (2002), “Design and Construction of Externally Bonded FRP Systems for Strengthening Concrete Structures (ACI 440.2R-02)”, *American Concrete Institute*. Farmington Hills, USA.
- Braga, F., Gigliotti, R. and Laterza, M. (2006), “Analytical Stress-strain relationship for concrete confined by steel stirrups and/or FRP jackets”, *ASCE Journal of Structural Engineering*, Vol. 132, No. 9, Pages 1402–1416.

Daniel, I.M. and Ishai, O. (2006), “Engineering Mechanics of Composite Materials”, *Oxford University Press*, New York, USA.

Eid, R. and Paultre, P. (2007), “Plasticity-based model for circular concrete columns confined with fibre-composite sheets”, *Journal of Engineering Structures*, Vol. 29, No. 12, Pages 3301–3311.

Elwi, A.A. and Murray, D.W. (1979), “A 3-D hypoelastic concrete constitutive relationship”, *Journal of Engineering Mechanics Division, ASCE*, Vol. 105, No. 4, Pages 623–641.

Fam A.Z. and Rizkalla S.H. (2001a), “Confinement Model for Axially Loaded Concrete Confined by FRP Tubes”, *ACI Structural Journal*, Vol. 98, No. 4, Pages 451-461.

Fam, A.Z. and Rizkalla, S.H. (2001b), “Behavior of Axially Loaded Concrete-Filled Circular Fiber-Reinforced Polymer Tubes”, *ACI Structural Journal*, Vol. 98, No. 3, Pages 280-289.

Jiang, T. and Teng, J.G. (2007), “Analysis-oriented stress-strain models for FRP-confined concrete”, *Journal of Engineering Structures*, Vol. 29, No. 11, Pages 2968–2986.

Kawashima, K., Hosotani, M., and Hoshikuma, J. (1997), “A model for confinement effect for concrete cylinders confined by carbon fiber sheets” *NCEER-INCEDE Workshop on Earthquake Engineering*, Frontiers of Transp. Fac., National Center for Earthquake Engineering Research, State University of New York, Buffalo, USA.

Lignola, G.P., Prota, A., Manfredi, G. and Cosenza, E. (2007a), “Experimental performance of RC hollow columns confined with CFRP”, *ASCE Journal of Composites for Construction*, Vol. 11, No. 1, Pages 42-49.

Lignola, G.P., Prota, A., Manfredi, G. and Cosenza, E. (2007b), “Deformability of RC hollow columns confined with CFRP”, *ACI Structural Journal*, Vol. 104, No. 5, Pages 629-637.

Lignola, G.P., Prota, A., Manfredi, G. and Cosenza, E. (2008b), “Unified Theory For Confinement of RC Solid and Hollow Circular Columns”, *ELSEVIER Composites part B*, Vol. 39, No. 7-8, Pages 1151-1160.

Lignola, G.P., Prota, A., Manfredi, G. and Cosenza, E. (2008c), “Non linear modeling of RC hollow piers confined with CFRP”, *ELSEVIER Composites Structures*, Vol. 88, No. 1, Pages 56-64.

Lignola, G.P., Prota, A., Manfredi, G. and Cosenza, E. (2008a), “Effective Strain in FRP Jackets on Circular RC Columns”, *4th International Conference on FRP Composites in Civil Engineering (CICE2008)*, Zurich, Switzerland, Paper No. 2.A.5.

Mander, J.B., Priestley, M.J.N. and Park, R. (1988), “Theoretical stress–strain model for confined concrete”, *ASCE Journal of the Structural Division*, Vol. 114, Pages 1804–1826.

Modarelli, R., Micelli, F. and Manni, O. (2005), “FRP-Confinement of Hollow Concrete Cylinders and Prisms”, *ACI SP-230-58*, Vol. 230, No. 2, Pages 1029-1046

Schickert, G. and Winkler, H. (1977), “Results of test concerning strength and strain of concrete subjected to multi-axial compressive stress”, *Deutsche Ausschuss für Stahlbeton*, Vol. 277, Berlin, West Germany, Page 123.

Spoelstra, M.R. and Monti, G. (1999), “FRP-confined concrete model”, *ASCE Journal of Composites for Construction*, Vol. 3, No. 3, Pages 143-150.

Teng, J.G., Huang, Y.L., Lam, L. and Ye, L.P. (2007), “Theoretical model for fiber reinforced polymer-confined concrete”, *ASCE Journal of Composites for Construction*, Vol. 11, No. 2, Pages 201-210.

William, K.J. and Warnke, E.P. (1975), “Constitutive Model for the Triaxial Behavior of Concrete”. *International Association for Bridge and Structural Engineering Proceedings*, 19.